Characterization of monomeric and gemini cationic amphiphilic molecules by fluorescence intensity and anisotropy. Part 2

Nadia Barbero, Pierluigi Quagliotto, Claudia Barolo, Emma Artuso, Roberto Buscaino, Guido Viscardi*

Department of General Chemistry and Organic Chemistry and NIS, Interdepartmental Centre of Excellence, University of Torino, C.so M. d' Azeglio 48, I-10125 Torino, Italy

ARTICLE INFO

ABSTRACT

Four fluorophores of different nature, structure and properties were employed as probes for the characterization of a series of alkanediyl-α,ω-bis(alkyldimethyl ammonium bromide) surfactants. Pyrene and 3-(2-Benzothiazolyl)-7-(diethylamino)coumarin (coumarin 6) fluorescence intensity as well as coumarin 6 and fluorescein sodium salt fluorescence anisotropy were used to determine cmc whilst coumarin 6, fluorescein sodium salt and perylene fluorescence anisotropy was exploited to provide information on micellar structure; cmc values were confirmed using conductivity measurements. Conductivity data were analysed by means of a method which reveals the formation of ion pairs or premicellar aggregates; this approach was useful to justify and confirm results obtained using fluorescence.

1. Introduction

Gemini surfactants contain two hydrophobic and two hydrophilic groups in the molecule, which are connected by a linkage of variable length close to the hydrophilic groups [1]. Ammonium gemini surfactants were thoroughly studied and used for practical applications, namely the preparation of mesoporous materials [2–4], the preparation of multi-walled carbon nanotubes [5], gene transfection by formation of the DNA/surfactant complexes [6], the solubilisation of oily and solid compounds [7], the emulsification of monomers for polymerizations [8].

In a recent paper [9] the authors proposed the use of fluorescein sodium salt for cmc determination, based on the fluorescence anisotropy of the dye. Moreover, the anisotropy of fluorescein sodium salt and another fluorescent probe, namely perylene, clarified the formation of micelles and provided a qualitative indication of the micellar surface compactness and core viscosity.

This work extends the use of fluorescence anisotropy for cmc determination and micellar studies to other surfactants by using another fluorophore namely, 3-(2-Benzothiazolyl)-7-(diethylamino)coumarin (coumarin 6) and a different conductivity approach. The surfactants used (Fig. 1) comprised two monomeric

surfactants, dodecyltrimethylammonium bromide (DTAB) and cetyltrimethylammonium bromide (CTAB) as well as a series of alkanediyl-α, ω-bis(alkyldimethyl ammonium bromide) surfactants, referred to as *16-n-16 2Br*, where *16* and *n* (*n* = 3, 4, 6, 10 and 12) are the carbon numbers of the surfactant alkyl chain and of the alkanediyl (polymethylene) spacer group, respectively and Br stands for bromide.

The fluorophores used are reported in Fig. 2; it is noteworthy that pyrene and coumarin 6 (C6) were used for cmc determination employing fluorescence intensity, both fluorescein sodium salt and C6 for cmc determination via anisotropy, while perylene and all fluorophores were used for micellar compactness determination. Fluorescein sodium salt is an anionic probe which is micellized, through electrostatic interactions, at the positively charged cationic micellar surface. Consequently, changes in the fluorescence anisotropy of fluorescein solubilised in cationic micellar solutions will reflect changes at the micellar surface [10]. In fact, spectroscopic studies previously reported [11] have shown that fluorescein is solubilised in the inner part of the Stern region of CTAB micelles. On the contrary, coumarin 6 is a neutral probe whose fluorescent properties in homogeneous and micellar media have been previously reported [12]. According to its spectral characteristics, it can be inferred that C6 is solubilised in the palisade layer of cationic surfactants micelles. Finally, perylene is solubilised in inner hydrocarbon region [11]. Since the three probes are located in different positions in the micelle the use of fluorescence anisotropy

* Corresponding author. Tel.: +39 011 6707598; fax: +39 011 6707591.
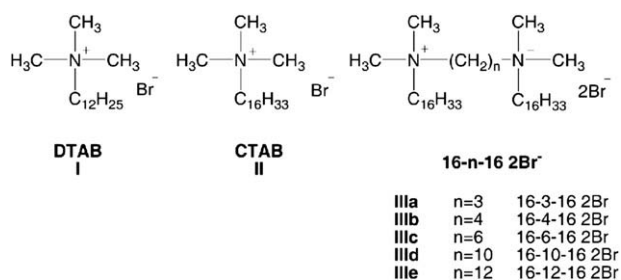E-mail address: guido.viscardi@unito.it (G. Viscardi).

Fig. 1. Structures of the studied surfactants.

technique can provide qualitative information that can be related to the micellar compactness and microenvironmental constraints of the micellar probe solubilisation site.

2. Experimental section

2.1. Materials

CTAB, pyrene, fluorescein sodium salt, perylene and coumarin 6 were purchased from Fluka while DTAB was purchased from Sigma Aldrich. Pyrene, fluorescein sodium salt, perylene and coumarin 6 were fluorescent grade; all chemicals were used as received without further purification.

Gemini surfactants were synthesized from the reaction of α,ω-dibromoalkanes with N,N,N-hexadecyldimethylamine as reported by Zana et al. [13,14]. The purity of the surfactants was checked using ^{1}H NMR, TLC (Thin Layer Chromatography) and LC-MS Mass Spectrometry.

2.2. Conductivity measurements

Conductivity measurements were performed on a conductivity meter equipped with a conductivity cell having cell constant of 0.943 cm^{-1} as already reported [15]. The addition of concentrated surfactant solution by a titrator and the collection of the conductivity data were performed by using a computer controlled automated system, working with a program written in Quick Basic, available from the authors. Water of MilliQ quality (conductivity: 0.05 μS; surface tension: 72.8 mN/m at 20 °C) was used for the measurements.

2.3. Fluorescence measurements

The steady-state intensity and anisotropy fluorescence measurements were performed on a Perkin Elmer LS 55 spectrofluorimeter. Pyrene stock solution was prepared by dissolving 5.3 mg of pyrene in 10 ml of methanol and 0.5 ml of this solution were diluted to 10 ml; perylene stock solution was prepared by dissolving 3.3 mg of perylene in 10 ml of ethanol and 0.25 ml of this solution were diluted to 10 ml; fluorescein stock solution was prepared by dissolving 3.9 mg of fluorescein in 10 ml of water and 1 ml of this solution was diluted to 5 ml; coumarin 6 stock solution was prepared by dissolving 3.1 mg of coumarin 6 in 10 ml of ethanol and 0.5 ml of this solution were diluted to 10 ml 10 μl of the probe stock solution

were added to the sample solutions prepared by dilution of the different surfactants stock solutions. Pyrene spectra were collected in the 360–600 nm range, checking carefully that no excimer was formed: final concentration 5×10^{-7} M, excitation wavelength 320 nm; excitation slit 5 nm and emission slit 2.5 nm; coumarin 6 spectra were collected in the 475–650 nm range, final concentration 1.5×10^{-7} M, excitation wavelength 465 nm; excitation slit 2.5 nm and emission slit 5.0 nm. The anisotropy settings were: a) fluorescein: final concentration 5×10^{-8} M, excitation wavelength 491 nm; emission wavelength 523 nm; excitation slit 2.5; emission slit 2.5 nm, integration 5 s; b) perylene: final concentration 3.5×10^{-7} M, excitation wavelength 412 nm; emission wavelength 472 nm; excitation slit 2.5; emission slit 5.0 nm, integration 5 s; c) coumarin 6: final concentration 1.5×10^{-7} M, excitation wavelength 465 nm; emission wavelength 505 nm; excitation slit 2.5; emission slit 5.0 nm, integration 5 s. Measurements were taken until equilibrium was attained. As for anisotropy measurements for the micellar structure investigation, the surfactant solutions had a concentration ten times the estimated cmc value. To these solutions, 10 μl of an ethanolic solution of perylene or coumarin 6 or an aqueous solution of fluorescein sodium salt were added.

3. Results and discussion

3.1. Conductivity

Critical micellar concentration (cmc) and degree of counterion binding (β) were obtained as a result of conductivity measurements and are reported in Table 1. Conductivity data are normally reported as specific conductivity (κ) vs. surfactant concentration (C) plot (see Fig. 3) or as molar conductivity (Λ) vs. $C^{0.5}$ plots (see Fig. 4). Cmc can be easily detected in the first kind of plot, due to an evident discontinuity. However, the second approach (Λ vs. $C^{0.5}$ plots) is useful in evidencing peculiarities that can be interpreted as due to the formation of ion pairs and/or premicellar aggregates [14].

3.1.1. Critical micellar concentration

The cmc values were obtained from κ vs. (C) plots by the intersection of the lines fitted in the diluted and concentrated regions before and after the cmc. The evaluation of the degree of counterion dissociation α and of counterion binding β ($\beta = 1-\alpha$) was carried out as the ratio of the slope of the lines graphically fitted in the premicellar and postmicellar ranges, respectively. Since for gemini surfactants the shape of the plots is smooth (Fig. 3) and the lines are quite difficult to be precisely defined, we also used a different approach in the data analysis based on a non linear fit introduced by Carpena et al. [16] which we already successfully applied to elaborate conductivity data obtained on gemini ammonium [9] and gemini pyridinium surfactants [17,18].

In Table 1 cmc and β values for both monomeric and gemini surfactants obtained by the two methods are reported and are in agreement with conductivity data found in literature [13–15,19,31].

Fig. 2. Structures of the used fluorophores.

Table 1
Summary of the results obtained by conductivity.

Compound	Classical method		Non linear fit		Literature	
	cmc (mM)	β (%)	cmc (mM)	β (%)	cmc (mM)	β (%)
DTAB (**I**)	14	79	14.3	78	16 [19]	77 [14]
CTAB (**II**)	0.955	82	0.936	81	0.92 [19]	84 [14]
16-3-16 (**IIIa**)	0.0265	64	0.0251	64	0.025 [13]	61 [13]
16-4-16 (**IIIb**)	0.0306	69	0.0268	71	0.027 [13]	44 [13]
16-6-16 (**IIIc**)	0.0519	61	0.0443	67	0.043 [13]	67 [15]
16-10-16 (**IIId**)	0.0336	69	0.0299	71	0.027 [31]	57 [13]
16-12-16 (**IIIe**)	0.0316	50	0.0209	73	0.020 [31]	

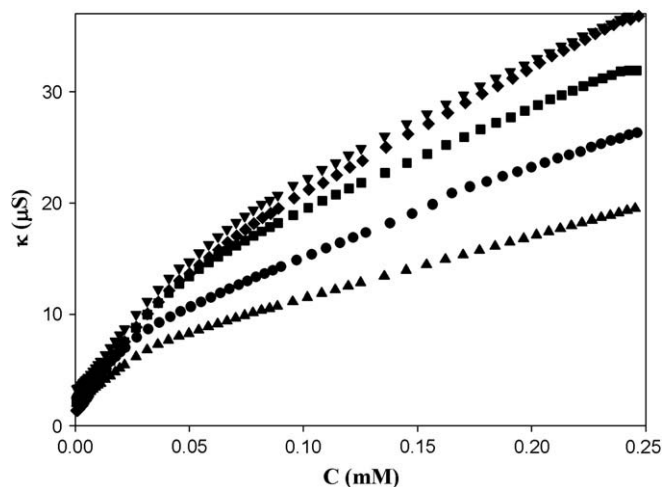**Fig. 3.** Specific conductivity (κ) vs. concentration for ● 16-3-16 2Br, ▲ 16-4-16 2Br, ■ 16-6-16 2Br, ▼ 16-10-16 2Br and ◆ 16-12-16 2Br.

3.1.2. Conductivity plot shape

Formation of ion pairs and premicellar aggregates can be detected by inspection of conductivity plots. Ion pairs occurrence can be detected by the deviation of the κ vs. C and the Λ vs. $C^{0.5}$ plots, that should show a curvature towards the C (or the $C^{0.5}$) axis, well below the cmc concentration. Formation of ion pairs will
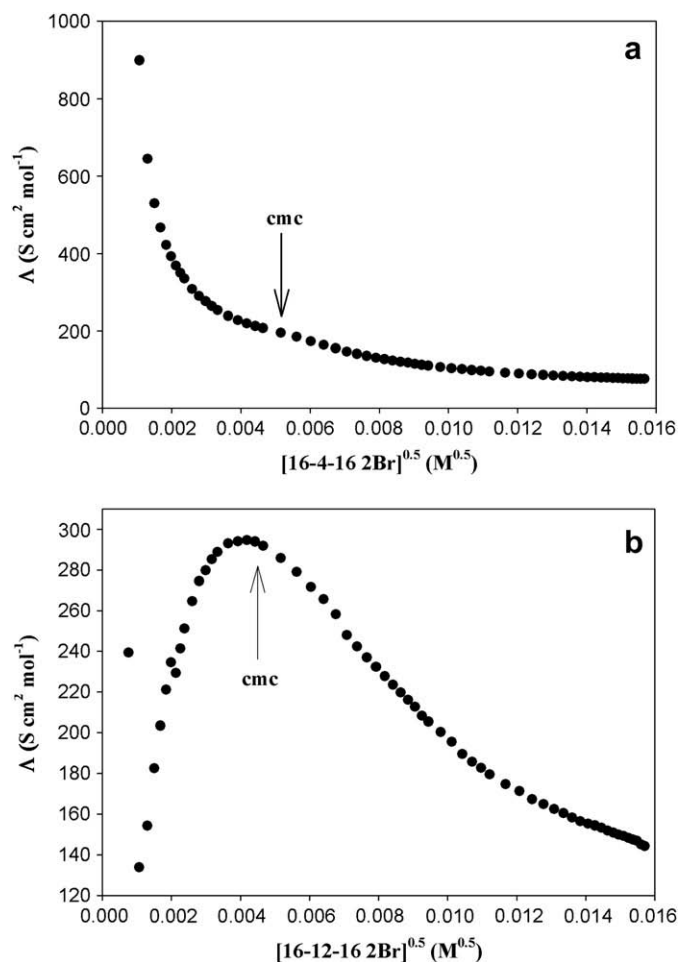

Fig. 4. Molar conductivity (Λ) vs. $C^{0.5}$ for a) 16-4-16 2Br and b) 16-12-16 2Br.

reduce the conductivity of the solution, due to the neutralization of electric charges and the slower diffusion of the ion pairs with respect to the separated ions. The formation of ion pairs is also expected to increase with increasing the surfactant concentration. On the contrary, premicellar aggregates are defined as surfactant aggregates of very low aggregation number. Their formation will result in a curvature, in the low concentration range, towards the κ axis, in the κ vs. C plots and in a maximum in Λ vs. $C^{0.5}$ plots. The appearance of a deviation from the conductivity predicted by the Onsager's law was found for gemini surfactants of this series having short spacer [14] and for other cationic surfactants [18]. All the present studied surfactants showed ion pairs formation (Fig. 4a) except for 16-10-16 2Br and 16-12-16 2Br which form premicellar aggregates as evidenced by the presence of a maximum in Λ vs. $C^{0.5}$ plot as shown in Fig. 4b as an example for spacer 12 (**IIIe**).

3.2. Fluorescence intensity of pyrene and coumarin 6

The pyrene (benzophenanthrene) use as fluorescent probe has been widely reported in the literature [20–22] to study surfactants aggregation. Pyrene emission characteristics are considered to estimate the polarity level of its solubilisation environment and this peculiarity was applied to monitor the micelles formation in solution. The resultant plots of the pyrene I_1/I_3 ratio as a function of the total surfactant concentration show, around the cmc, a typical sigmoidal decrease. The cmc determination was accomplished by using a recent approach [23] based on the assumption that the pyrene I_1/I_3 ratio plots can be adequately described by a decreasing sigmoid of the Boltzmann type, which is given by equation (1):

$$y = \frac{A_1 - A_2}{1 + e^{(x-x_0)/\Delta x}} + A_2 \tag{1}$$

where the variable y corresponds to the pyrene I_1/I_3 ratio value, the independent variable x is the total concentration of surfactant, A_1 and A_2 are the upper and lower limits of the sigmoid, respectively, x_0 is the centre of the sigmoid, and Δx is directly related to the independent variable range where the abrupt change of the dependent variable occurs.

As already reported in our previous work [9], the shape of the plots shows a typical sigmoidal decrease for both monomeric (DTAB and CTAB) and gemini surfactants having short spacer (16-3-16 and 16-4-16 2Br). On the contrary, when the spacer is longer than $n = 6$, the plot shape is highly distorted. Two examples of sigmoidal and distorted sigmoidal plots are reported in Fig. 5. The results obtained by sigmoidal fit of the well-behaving plots gave results in very good agreement with those of conductivity (compare Table 1 and Table 2). However, as already pointed out [9] the concentration range in which the micellization phenomena occur is always quite large for gemini while the two monomers, i.e. DTAB and CTAB, gave more definite transitions. On the contrary, the application of the sigmoidal fit to the distorted plots gave results slightly different from those obtained by conductivity. The distorted plots were already showed by Zana et al. [24], for 14-2-14 and 16-2-16 2Br for which the cmc determined by fluorescence was greater than that found by conductivity. This was exactly what we found for the compounds giving distorted sigmoidal plots.

I_1/I_3 value measures the wetting/dewetting of pyrene solubilisation site and follow the reverse order of the degree of counterion binding. The I_1/I_3 value, when the micellization process is concluded (see Table 3), suggests that the micelle shape and/or micellar surface compactness influence significantly the pyrene solubilisation site; consequently, the probe senses a different polarity in the different micelles. I_1/I_3 values show that there is also some dependence of the polarity of micelle on the spacer length for
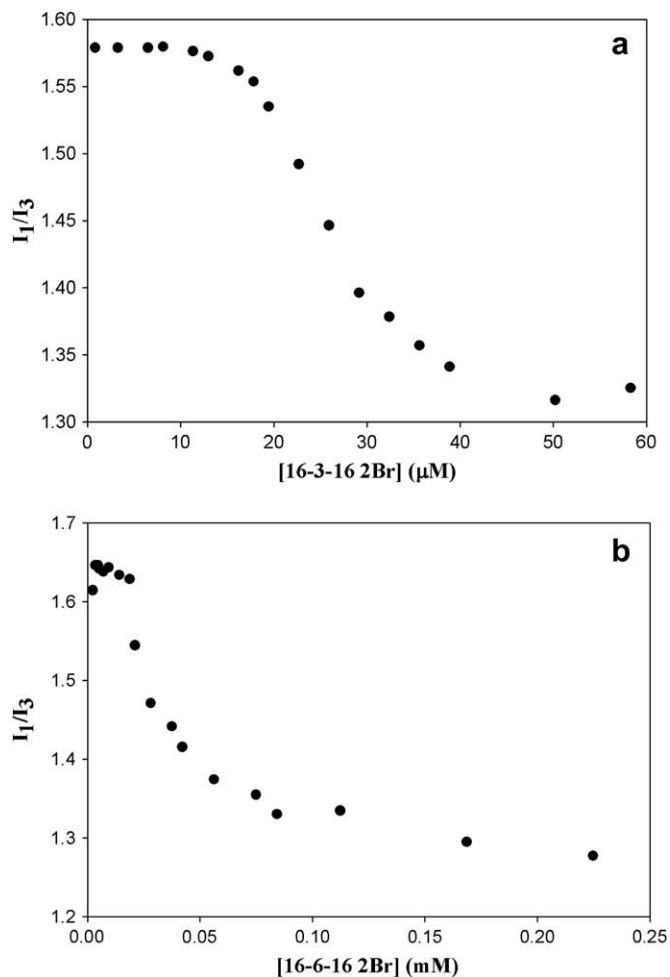
Fig. 5. Plot of the fluorescence pyrene I_1/I_3 intensity ratio vs. concentration, a) data for 16-3-16 2Br and b) data for 16-6-16 2Br.

gemini surfactants. Pyrene will be located in different part of the micelle, depending on the spacer length. Longer spacers can account for a more interior location of the probe: the spacer folds towards the interior of the micelle making the palisade zone more hydrophobic.

Cmc values for all the studied surfactants (**I**, **II**, **IIIa–e**) have also been obtained by using coumarin 6 fluorescence intensity and data are reported in Table 2. As already found for pyrene fluorescence, monomeric and short spacer surfactants show a sigmoidal behaviour which becomes distorted for longer spacers as reported in Fig. 6 for 16-10-16 2Br as an example. It is noteworthy to say that,

Table 2
Summary of the results obtained by (a) fluorescence intensity and (b) fluorescence anisotropy.

Compound	Pyrene[a]	Coumarin 6[a]	Fluorescein[b]	Coumarin 6[b]	Literature
	cmc (mM)	cmc (mM)	cmc (mM)	cmc (mM)	cmc (mM)
DTAB (**I**)	14.9	15.6	14.2	13	16 [19]
CTAB (**II**)	0.987	0.87	0.948	0.882	0.92 [19]
16-3-16 (**IIIa**)	0.026	0.026	0.026	0.034	0.025 [13]
16-4-16 (**IIIb**)	0.027	0.029	0.029	0.027	0.027 [13]
16-6-16 (**IIIc**)	0.020	0.044	–	0.043	0.043 [13]
16-10-16 (**IIId**)	0.029	0.026	–	–	0.027 [31]
16-12-16 (**IIIe**)	0.024	0.023	–	–	0.020 [31]

[a] from fluorescence intensity.
[b] from fluorescence anisotropy.

even if the shape of the plots resulted distorted, the evaluation of the cmc was possible and the obtained values are in agreement with data found by different methods and those reported in literature. The fact that, for longer spacers, plots are distorted could be due to the formation of surfactants premicellar aggregates with the probe favoured by the presence of long hydrophobic spacers [14].

3.3. Fluorescence anisotropy

Anisotropy measurements [25] are based on the molecular motion of fluorescent molecules in solution in the time window occurring between absorption and emission of light. According to equation (2), the fluorescence anisotropy (r) values were determined as:

$$r = \frac{I_{vv} - GI_{vh}}{I_{vv} + 2GI_{vh}} \tag{2}$$

where I_{vv} and I_{vh} represent the vertically and horizontally polarized emission intensities, respectively, following instrumental excitation with vertically polarized light and G is a correction factor which detects the instrumental sensitivity of the polarization direction of emission. G is defined as $G = I_{hv}/I_{hh}$, where I_{hv} and I_{hh} represent the vertically and horizontally polarized emission intensities obtained by excitation with horizontally polarized light.

3.3.1. Cmc determination by fluorescence anisotropy of fluorescein sodium salt and coumarin 6

Several phenomena can decrease the measured anisotropy: the most common one is the probe rotational diffusion, which occurs during the lifetime of the excited state and displaces the emission dipole of the fluorophore. In this work we applied this simple principle for the determination of the cmc taking into account that: 1) if a fluorescent probe is added to a surfactant solution whose concentration is below the cmc, the measured anisotropy will be low due to the fact that the fluorophore will remain in the water phase and will have a high rotational rate; 2) when the surfactant solution reaches a concentration at which the micelles start to form (i.e. at the cmc), the anisotropy will obviously increase because the rotational diffusion of the probe will be decreased owing to the constraints inside the micelles.

Since fluorescence anisotropy comes out from the restriction of the mobility of the probe during the light absorption and light emission events, it seems reasonable to relate the anisotropy of the micellar state, if a constant value can be obtained, to a restricted environment where the probe is located.

Fluorescein sodium salt and coumarin 6 fluorescence anisotropy was used for the determination of the cmc of the above mentioned surfactants. Sigmoidal fitting of the experimental points gave excellent results from both the plot shape and the cmc values point of view only for monomeric and short spacer surfactants as for fluorescence intensity measurements. The cmc values for DTAB and CTAB and gemini with spacer 3 and 4 (**IIIa** and **IIIb**) are in excellent agreement with data obtained by conductivity and fluorescence intensity and with literature as reported in Table 2. An exception is for $n = 3$ (**IIIa**) for which C6 is overestimating the cmc value even if the graphical behaviour is perfectly sigmoidal. On the contrary, there is a deviation from sigmoidal behaviour for gemini with spacer > 6 as it is evidenced in Fig. 7a for 16-10-16 2Br with fluorescein where the absence of the plateau at low surfactant concentration is clear. Besides, for C6 measurements for surfactants with longer spacer, the complete absence of the plateau at low concentration is accompanied by the lack of a stable plateau at higher concentration, above the cmc (see. Fig. 7b). The fact that the anisotropy increases at a very low concentration is an evidence of

Table 3
Summary of the results obtained by pyrene fluorescence intensity and anisotropy of fluorescein sodium salt, coumarin 6 and perylene.

Compound	Pyrene	Fluorescein			Coumarin 6			Perylene		
	I_1/I_3[a]	r^*	S	Θ	r[a]	S	Θ	r[a]	S	Θ
DTAB (**I**)	1.26	0.061	0.179	73.72	0.142	0.485	52.81	0.013	0.036	86.08
CTAB (**II**)	1.23	0.100	0.311	64.26	0.169	0.575	49.93	0.017	0.048	84.92
16-3-16 (**IIIa**)	1.33	0.120	0.380	59.66	0.226	0.737	35.60	0.037	0.110	79.30
16-4-16 (**IIIb**)	1.32	0.134	0.428	56.54	0.216	0.711	37.50	0.028	0.082	81.79
16-6-16 (**IIIc**)	1.35	0.138	0.441	55.65	0.211	0.698	38.47	0.029	0.085	81.51
16-10-16 (**IIId**)	1.23	0.100	0.311	64.26	0.200	0.668	40.61	0.026	0.075	82.35
16-12-16 (**IIIe**)	1.21	0.075	0.226	70.26	0.199	0.665	40.81	0.025	0.072	82.64

[a] I_1/I_3 and r measured when the micelle formation is completed.

a strong mobility reduction of the probe which could be caused by several phenomena: aggregation of the probe with itself, with the micelle or with the surfactant. We can exclude the self aggregation since the probe concentration is very low and constant and identical for every experiment. We can also exclude the aggregation with the micelles since, according to conductivity data, micelles are not yet formed at this concentration. However, as already reported in Section 3.1.2, conductivity measurements show the presence of premicellar aggregates for gemini with long spacer. The hypothesis of premicellar aggregates formation is in agreement with the distorted shape of plots reported for C6 and fluorescein anisotropy for surfactants with longer spacer. This hypothesis is enforced since the plot shape distortion is not occurring for short spacer gemini surfactants, where premicellar aggregates are not present.

As already reported in our previous work [9] and as also detected by fluorescence intensity measurements in the present work, for gemini surfactants, the concentration range (Δx) where the transition between the premicellar and the micellar state occurs is larger than that observed for monomeric surfactants. This different behaviour, which is also observed by comparing data obtained by other techniques, could be correlated to a greater difficulty in the micelles formation for gemini surfactants: a gradual micellization process occurs because of the difficulty of arrangement of two hydrophobic chains per molecule in the micellar core.

3.3.2. Fluorescence anisotropy of fluorescein sodium salt, perylene and coumarin 6 for micellar structure investigation

The motion of probe molecules in an anisotropic environment can be described in terms of the wobbling in cone model [26]. According to this model the rotation of a molecule probe can undergo free rotational diffusion within a cone of semiangle θ_C,

known as the critical angle. Another important parameter in this model is the so-called order parameter, S, which provides a measure of the equilibrium orientational distribution of the probe and which decreases with increasing mobility of the dye in the medium. The critical angle, θ_C, and the order parameter, S, are related by equation (3) [27]:

$$S = \frac{1}{2}\cos\,\theta_C(1 + \cos\,\theta_C) \tag{3}$$

Based on semiempirical considerations, Pottel et al. [28] have obtained a relationship between S and steady-state fluorescence anisotropy given by equation (4):
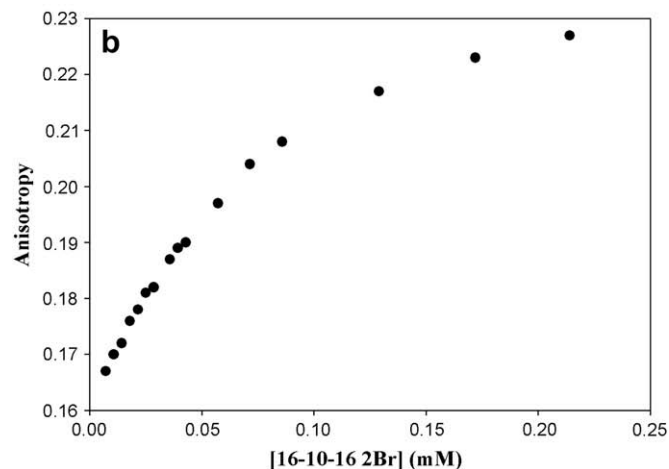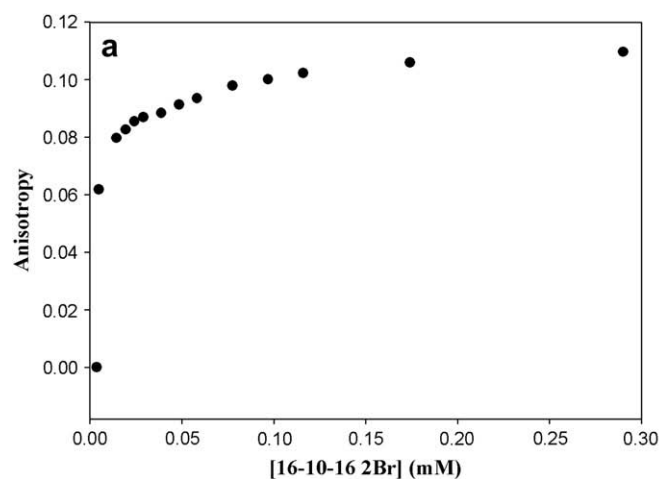

Fig. 6. Plot of the coumarin 6 fluorescence intensity vs. concentration, data for 16-10-16 2Br.

Fig. 7. (a) Plot of the fluorescence anisotropy of a) fluorescein sodium salt vs. concentration for 16-10-16 2Br and b) coumarin 6 vs. concentration for 16-6-16 2Br.
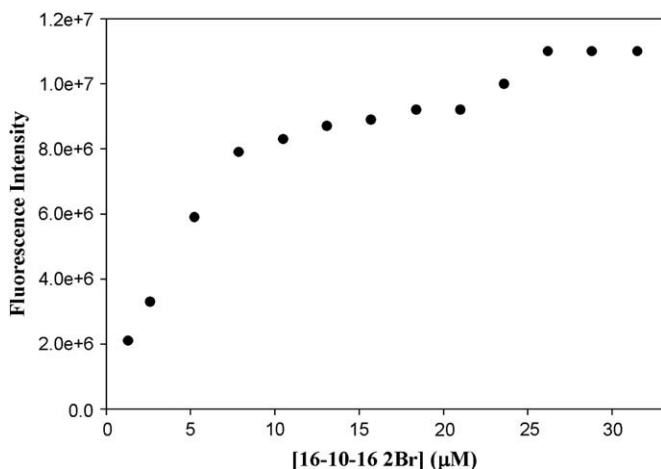
$$\frac{r}{r_0} = \frac{S}{1 + S - S^2} \qquad (4)$$

which makes it possible to determine the S value, and hence θ_C, from steady-state fluorescence anisotropy. In equation (4), r is the measured anisotropy and r_0 is the limiting anisotropy (0.390 for fluorescein [29], 0.329 for coumarin 6 [30] and 0.370 for perylene [10]) obtained in the absence of rotational motion, determined at low temperature in viscose solutions.

Fluorescence anisotropy can qualitatively give information on the micellar compactness and can help in making hypothesis on micelles shape. Actually, if other literature data are available, or if a deeper investigation using particular techniques (SANS, Cryo-TEM studies or dynamic light scattering) is performed, fluorescence anisotropy can confirm micellar structures and compactness. Three probes such as fluorescein sodium salt, perylene and coumarin 6 were taken into account in order to monitor the different probes mobility in different areas of the micelle. Fluorescein sodium salt, being an anionic probe, is located in the palisade region, in particular in the inner part of the Stern region. Perylene is located in the inner hydrocarbon region, i.e. in the micellar core while coumarin 6 is in the palisade region, as reported in Fig. 8. These three probes have been selected because they are suitable for fluorescence anisotropy measurements since they present high limiting anisotropy values, high fluorescence quantum yields and low fluorescence lifetimes (in order to prevent significant contributions from micellar rotation to the overall anisotropy) [10,25].

As reported in Table 3, the anisotropy values obtained for the micellar state are increasing when the chain is lengthened, i.e. from DTAB to CTAB, suggesting that a more compact and rigid micellar structure is obtained. By comparing CTAB and 16-3-16, i.e. the monomer and a gemini surfactant, a similar behaviour is shown, evidencing that in gemini surfactants micelles the probe mobility is more restricted. This is in agreement with SANS evidences [31] of large prolate ellipsoidal structures for 16-n-16 (n = 3, 4). This could account for the higher restriction of the probe mobility since those arrangements are more compact at the micellar surface than spherical micelles typical for CTAB like surfactants. Moreover, the

anisotropy data, recorded at ten times the cmc, show that there is an increase of the r value for the 16-n-16 2Br series up to n = 6. Data in Table 3 also indicate that the order parameter, S, is in a complete agreement with these data and shows a gradual increase, whereas the critical angle decreases, up to n = 6 indicating that the probe is sensing a more constrained environment. This decreases for longer spacers ($n > 6$) indicating that the micelle shape is changing towards micelles which are similar to those of monomeric surfactants.

We can recall from literature that, at these working concentrations (ten times the cmc), CTAB and DTAB form spherical micelles [32], while 16-3-16 2Br [33] and 16-4-16 2Br [31,34] present rod-like micelles. On the contrary, longer spacers surfactants should form prolate ellipsoidal as reported by Aswal et al. [34].

In a qualitative way the micellar anisotropy values can indicate that short spacer gemini aggregates could not have a spherical shape since the r values for geminis are higher with respect to monomers for which the probe can rotate more easily in a spherical structure. The similar r value obtained for monomeric and for gemini with longer spacer could indicate that these micelles have a similar shape, i.e. a looser micellar structure, nearly spherical or spheroidal.

Perylene anisotropy monitors the probe mobility restriction in the micellar core. The micellar core appears more compact when the chain is longer (see DTAB vs. CTAB), and for gemini surfactants (see CTAB vs. 16-3-16 2Br), probably due to a higher compactness of the core, which is usual for geminis. While being small, the difference for both fluorescein and perylene anisotropy for 16-3-16 2Br and 16-4-16 2Br surfactants seems to indicate a more compact micellar surface for 16-4-16 2Br vs. 16-3-16 2Br and, at the same time, a higher fluidity of the micellar core by lengthening the spacer. In a few words, the probe mobility in the micellar core is raised when the spacer is longer, while the reverse is observed for the micellar surface, in qualitative agreement with the change of micellar shape. This means that the micellar surface compactness is increasing up to 16-6-16 2Br and decreases for the longer spacers (n = 10, 12), while the micellar core is progressively becoming more fluid as a result of higher probe mobility.

4. Conclusions

The amphiphilic properties of a series of alkanediyl-α,ω-bis(alkyldimethyl ammonium bromide) and two monomeric surfactants have been studied by conductivity and fluorescence measurements.

Pyrene and coumarin 6 fluorescence intensity along with coumarin and fluorescein sodium salt fluorescence anisotropy have demonstrated to be successful methods for the determination of cmc of two monomeric and short spacer gemini surfactants. Actually, for these compounds (DTAB, CTAB and gemini up to spacer = 6) the sigmoidal plot shape is excellent and the agreement with results obtained by conductivity measurements is very good. By the lengthening of the spacer, a distortion from sigmoidal behaviour is detected and the determination of the cmc becomes more difficult. This is explained by the presence of premicellar aggregates which have also been confirmed by means of molar conductivity.

The different nature, structure and location of the used fluorophores and the comparison of our results with literature data helped us in a qualitative understanding of the surface compactness of the studied micelles. The limits found for the determination of the cmc for long spacer surfactants were not found for the fluorescence anisotropy structure investigation. Thus, fluorescence anisotropy technique revealed a reliable and easy tool for the micellar structure investigation of all the studied cationic surfactants.
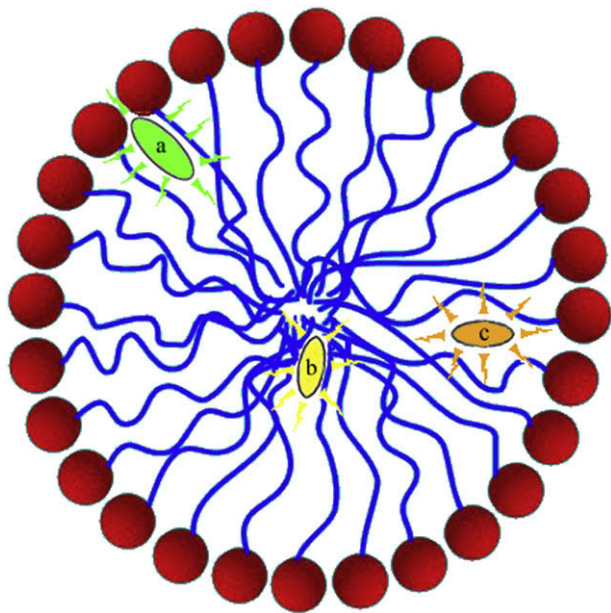

Fig. 8. Pictorial view of the different fluorophores location in the micelle: (a) fluorescein sodium salt near the headgroups, (b) perylene in the core and (c) coumarin 6 in the palisade zone.

Acknowledgments

References

[1] Rosen MJ. Surfactants and interfacial phenomena. 3rd ed. New York: Wiley-Interscience; 2004.
[2] Yu X, Xu Z, Han S, Che H, Yan X, Liu A. Synthesis of well-ordered lamellar mesoporous molybdenum oxide. Colloids Surf A Physicochem Eng Asp 2009;333:194–8.
[3] Huo Q, Margolese DI, Stucky GD. Surfactant control of phases in the synthesis of mesoporous silica-based materials. Chem Mater 1996;8:1147–60.
[4] Gianotti E, Berlier G, Costabello K, Coluccia S, Meneau F. In-situ Synchrotron small-angle X-ray scattering study of MCM-41 Crystallisation using gemini surfactants. Catal Today 2007;126:203–10.
[5] Chen L, Xie H, Li Y, Yu W. Applications of cationic gemini surfactant in preparing multi-walled carbon nanotube contained nanofluids. Colloids Surf A Physicochem Eng Asp 2008;330:176–9.
[6] Chen X, Wang J, Shen N, Luo Y, Li L, Liu M, et al. Gemini surfactant/DNA complex monolayers at the air–water interface: effect of surfactant structure on the assembly, stability, and topography of monolayers. Langmuir 2002;18:6222–8.
[7] Chen H, Han L, Luo P, Ye Z. The interfacial tension between oil and gemini surfactant solution. Surf Sci 2004;552:L53–7.
[8] Summers M, Kastoe J. Applications of polymerizable surfactants. Adv Colloid Interface Sci 2003;100-102:137–52.
[9] Quagliotto P, Barbero N, Barolo C, Costabello K, Marchese L, Coluccia S, et al. Characterization of monomeric and gemini cationic amphiphilic molecules by fluorescence intensity and anisotropy. Dyes Pigments 2009;82:124–9.
[10] Ruiz CC. Fluorescence anisotropy of probes solubilized in micelles of tetra-decyltrymethylammonium bromide: effect of ethylene glycol added. J Colloid Interface Sci 2000;221:262–7.
[11] Garcia-Sanchez F, Ruiz CC. Intramicellar Energy Transfer in aqueous CTAB solutions. J Lumin 1996;69:179–86.
[12] Ruiz CC, Díaz-López L, Aguiar J. Self-assembly of tetradecyl-trimethylammonium bromide in glycerol aqueous mixtures: a thermodynamic and structural study. J Colloid Interface Sci 2007;305:293–300.
[13] Zana R, Benrraou M, Rueff R. Alkanediyl-α,ω-(dimethylalkylammonium bromide) surfactants. 1. Effect of the spacer length on the critical micelle concentration and micelle ionization degree. Langmuir 1991;7:1072–5.
[14] Zana R. Alkanediyl-α,ω-bis(dimethylalkylammonium bromide) surfactants. 10. Behavior in aqueous solution at concentrations below the critical micellization concentration: an electrical conductivity study. J Colloid Interface Sci 2002;246:182–90.
[15] Viscardi G, Quagliotto P, Barolo C, Savarino P, Barni E, Fisicaro E. Synthesis and surface and antimicrobial properties of novel cationic surfactants. J Org Chem 2000;65:8197–203.
[16] Carpena P, Aguiar J, Bernaola-Galvan P, Ruiz CC. Problems associated with the treatment of conductivity-concentration data in surfactant solutions: simulations and experiments. Langmuir 2002;18:6054–8.
[17] Quagliotto P, Viscardi G, Barolo C, Barni E, Bellivia S, Fisicaro E, et al. Gemini pyridinium surfactants: synthesis and conductometric study of a novel class of amphiphiles. J Org Chem 2003;68:7651–60.
[18] Quagliotto P, Barolo C, Barbero N, Barni E, Compari C, Fisicaro E, et al. Synthesis and characterization of highly fluorinated gemini pyridinium surfactants. Eur J Org Chem 2009;2009(20):3167–77.
[19] Rosen MJ, Tracy DJ. Gemini surfactants. J Surfactants Deterg 1998;1: 547–54.
[20] Dominguez A, Fernandez A, Gonzalez N, Iglesias E, Montenegro L. Determination of critical micelle concentration of some surfactants by three techniques. J Chem Educ 1997;74:1227–31.
[21] van Stam J, Depaemelaere S, De Schryver C. Micellar aggregation numbers – a fluorescence study. J Chem Educ 1998;75:93–8.
[22] Kalyanasundaram K, Thomas JK. Environmental effects on vibronic band intensities in pyrene monomer fluorescence and their application in studies of micellar systems. J Am Chem Soc 1977;99:2039–44.
[23] Aguiar J, Carpena P, Molina-Bolivar JA, Ruiz CC. On the determination of the critical micelle concentration by the pyrene 1:3 ratio method. J Colloid Interface Sci 2003;258:116–22.
[24] Zana R, Levy H. Alkanediyl-α,ω-(dimethylalkylammonium bromide) surfactants (dimeric surfactants). Part 6. CMC of the ethanediyl-1,2-bis(dimethylalkylammonium bromide) series. Colloids Surf A Physicochem Eng Aspects 1997;127:229–32.
[25] Lakowicz JR. Principles of fluorescence spectroscopy. New York: Springer-Verlag; 2006.
[26] Kinosita K, Kawato S, Ikegami A. A theory of fluorescence polarization decay in membranes. Biophys J 1977;20:289–305.
[27] Lipari G, Szabo A. Effect of vibrational motion on fluorescence depolarization and nuclear magnetic resonance relaxation in macromolecules and membranes. Biophys J 1980;30:489–506.
[28] Pottel H, Van Der Meer W, Herreman W. Correlation between the order parameter and the steady-state fluorescence anisotropy of 1,6-diphenyl-1,3,5-hexatriene and evaluation of membrane fluidity. Biochim Biophys Acta 1983;730:181–6.
[29] Heitz MP, Bright FV. Rotational reorientation dynamics of Xanthene dyes within the interior of aerosol-OT reversed micelles. Appl Spectrosc 1995;49:20–30.
[30] Dutt GB, Raman S. Rotational dynamics of coumarins: an experimental test of dielectric friction theories. J Chem Phys 2001;114:6702–13.
[31] De S, Aswal VK, Goyal PS, Bhattacharya S. Role of spacer chain length in dimeric micellar organization. Small angle neutron scattering and fluorescence studies. J Phys Chem 1996;100:11664–71.
[32] Shikata T, Hirata H, Kotaka T. Micelle formation of detergent molecules in aqueous media: viscoelastic properties of aqueous cetyltrimethylammonium bromide solutions. Langmuir 1987;3:1081–6.
[33] Aswal VK, De S, Goyal PS, Bhattacharya S, Heenan RK. Transition from disc to rod-like shape of 16-3-16 dimeric micelles in aqueous solutions. J Chem Soc Faraday Trans 1998;94:2965–7.
[34] Aswal VK, De S, Goyal PS, Bhattacharya S, Heenan RK. Small-angle neutron scattering study of micellar structures of dimeric surfactants. Phys Rev E 1998;57:776–83.